A jellyfish-like swimming mini-robot actuated by an electromagnetic actuation system

2012 Smart Mater. Struct. 21 057001

(http://iopscience.iop.org/0964-1726/21/5/057001)

Smart Mater. Struct. **21** (2012) 057001 (9pp) doi:10.1088/0964-1726/21/5/057001

TECHNICAL NOTE

A jellyfish-like swimming mini-robot actuated by an electromagnetic actuation system

Youngho Ko, Sungyoung Na, Youngwoo Lee, Kyoungrae Cha, Seong Young Ko, Jongoh Park and Sukho Park

Department of Mechanical Engineering, Chonnam National University, Gwangju, 500-757, Korea

E-mail: jop@jnu.ac.kr and spark@jnu.ac.kr

Received 29 November 2011, in final form 23 February 2012
Published 24 April 2012
Online at stacks.iop.org/SMS/21/057001

Abstract

Among the various kinds of actuations for biomimetic robots, the electromagnetic actuation (EMA) method has been regarded as the one with the most potential. This paper proposes a jellyfish-like swimming mini-robot actuated by an EMA system in three-dimensional (3D) space. The jellyfish-like mini-robot has four flexible fins, each of which is equipped with a permanent magnet for electromagnetic actuation; the robot's body is 17 mm long and 0.5 mm thick. Our EMA system was able to generate a uniform magnetic field in a desired direction in 3D space, which could bend the fins of the jellyfish-like mini-robot. Therefore, a cyclic change in the uniform magnetic field, in the EMA system, would synchronize the fluctuation of the fins and could generate a propulsion force for the robot, in the desired direction. In order to maximize the propulsion force of the jellyfish-like mini-robot, the waveform and frequency of the input current in the EMA system are optimized. Consequently, our jellyfish-like mini-robot was able to generate maximum propulsion force when a square waveform input current (13 A magnitude and 10 Hz frequency) was applied to the EMA system. Finally, the jellyfish-like mini-robot with the EMA system was able to perform various 3D swimming motions.

(Some figures may appear in colour only in the online journal)

1. Introduction

Technologies mimicking organisms' abilities have been applied within various fields—the airplane was made by mimicking the wing, Velcro tape mimics the thistle, and, recently, adhesive protein mimics a mussel. Applying the inherent abilities of organisms to human technology is biomimetic engineering. In the field of biomimetic robots, swimming robots could have significant potential. With regard to the potential applications of swimming robots, there exist underwater monitoring applications, such as pollution detection, exploration of unstructured underwater environments, stomach capsule endoscopes, pipe inspection robots, and blood clot collection robots [1–3]. Because the jellyfish has a special appearance and unique swimming form, many researchers have been interested in it.

Jellyfish-like robots using different kinds of actuators have been studied. Guo reported a swimming jellyfish robot made using SMA (shape memory alloy) and ICPF (ionic conducting polymer–gel film) [3]. Oh used IPMC (ionic polymer metal composite) at low actuating voltage and mimicked the pulse and recovery motions of the jellyfish [4]. However, because these jellyfish-like robots produce small propulsion force and experience interference from the power supply wires, they were unable to execute free swimming motion in 3D space.

To compensate for the power wire problem, researchers have applied an external magnetic field to the robots. Guo proposed a fish robot consisting of a disk-type permanent magnet head and a thin film-type fin. A cylindrical coil tube produces an external magnetic field that makes the fin shake and propels the fish robot. However, the fish robot could move only along the coil tube [5]. Nelson proposed a bacterial flagellum microrobot powered by an external magnetic field. A rotational magnetic field was generated in order to rotate the spiral-shaped microrobot body and propel the microrobot [6]. Kosa proposed a swimming capsule endoscope with pulsating fins, generated by a modulated magnetic field from an external magnetic field [7]. However, because of its complex structure, the swimming capsule endoscope is difficult to miniaturize. We reported on a swimming tadpole robot using two pairs of Helmholtz coils. The planar Helmholtz coils system generates a uniform magnetic field with a desired strength, and in the desired direction, in the 2D plane. Because the tadpole robot consists of the head with a permanent magnet and the flexible tail fin made from PDMS polymer, it was able to carry out 2D swimming motions in the region of interest (ROI) [8]. Although these robots can be controlled wirelessly, by applying an external magnetic field, they were not able to carry out the basic swimming motion of a robot in 3D space.

This study proposes a jellyfish-like swimming mini-robot in 3D space, which is controlled by the external magnetic field from three pairs of Helmholtz coils. Firstly, the structure of the robot and the effects of the magnetic field were analyzed. On the basis of the simulation results, the robot and the EMA coil system were designed and fabricated. Through various experiments, the optimal swimming conditions (such as the form and frequency of the input current) in 3D space were adjusted. The swimming motion of the proposed jellyfish-like mini-robot was easily controlled using a conventional joystick and the LabVIEW program.

2. Fabrication of the EMA coil system and jellyfish-like swimming mini-robot

2.1. The EMA coil system

Generally, a pair of Helmholtz coils is used to generate a uniform magnetic field in the region of interest (ROI) [9]. When a permanent magnet is located in the uniform magnetic field generated by a Helmholtz coil, it rotates to align in the direction of the generated uniform magnetic field and the following torque (τ) is generated:

$$\boldsymbol{\tau} = V\mathbf{M} \times \mathbf{B} \tag{1}$$

where V and $\mathbf{M}$ represent the volume and magnetization of the permanent magnet, respectively, and $\mathbf{B}$ denotes the magnetic flux of the external magnetic field [10].

Generally, there are two kinds of Helmholtz coils: the circular-type and the rectangular-type ones. Compared with circular Helmholtz coils, rectangular coils have a larger ROI and swimming area. Therefore, three pairs of rectangular Helmholtz coils in the three axis directions (x-, y-, and z-axis) were introduced. These pairs of coils were used to generate a uniform magnetic field in the desired direction in 3D space. The proposed EMA coil system was fabricated, as shown in figure 1, and the detailed specifications of the Helmholtz coils are described in table 1.

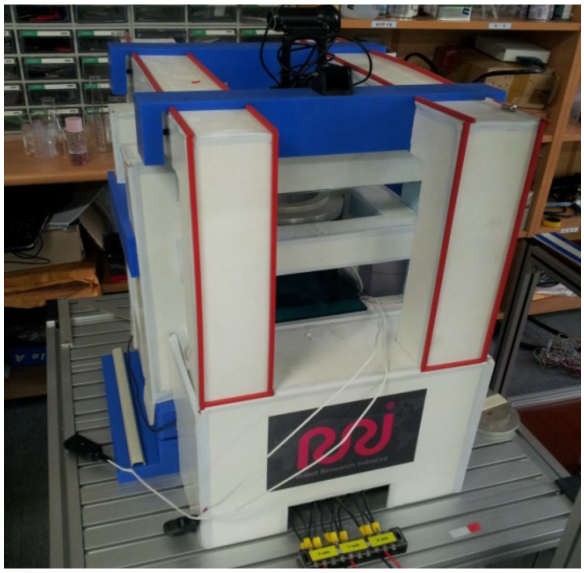

Figure 1. Three-axis rectangular Helmholtz coils.

Table 1. Specification of the 3D EMA system

	Helmholtz coil		
Coils	x	y	z
Radius (mm)	272.25	196.02	141.57
Coil turns	577	415	300
Diameter of copper wire (mm)	2	1.8	1.5

The rotational torque generated by the rectangular coil from equation (1) was calculated and B is also given as

$$B(z) = \frac{2\mu_0 iNa^2}{\pi}\left\{\frac{1}{[a^2+(z-d/2)^2]\sqrt{2a^2+(z-d/2)^2}} + \frac{1}{[a^2+(z+d/2)^2]\sqrt{2a^2+(z+d/2)^2}}\right\} \tag{2}$$

where i denotes the applied current, N the coil turns, a the half-size of the side of a square coil, μ_0 the permeability in a vacuum, z the distance between the coil centers, and d the distance between the coils [11, 12]. The detailed specification of the EMA system is described in table 2. Therefore, when the parameters in table 2 were applied, the magnetic flux in equation (2) was simplified to

$$B(z) = \mu_0(0.6481)\frac{i \times N}{a}. \tag{3}$$

As shown in figure 2, the desired direction is defined by the values of $\theta(\theta)$ and $\alpha(\alpha)$, and these values are controlled by means of a conventional joystick, PXI, and the LabVIEW program (National Instruments). With the desired direction, the current values (I_x, I_y, and I_z) of the EMA coil system could

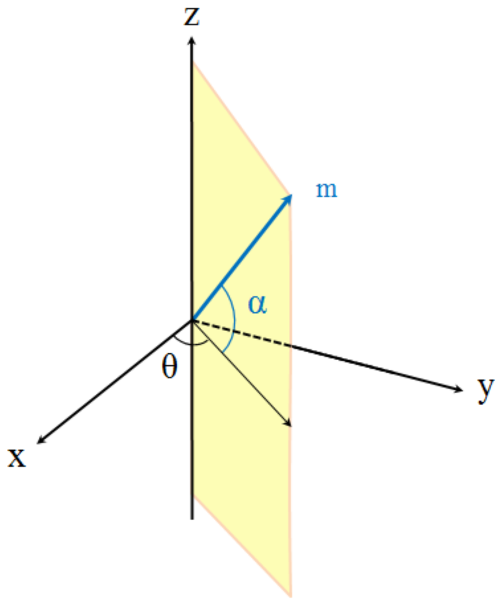

Figure 2. Desired direction of the robot.

be described as

$$\begin{bmatrix} I_x \\ I_y \\ I_z \end{bmatrix} = \begin{bmatrix} m\cos\alpha\cos\theta \\ m\cos\alpha\sin\theta \\ m\sin\alpha \end{bmatrix} \quad (4)$$

where m denotes magnetization magnitude of the desired direction. When these current component values are applied to the EMA coil system, all magnets in the ROI are aligned to the desired direction.

Table 2. Specification of the boundary condition.

Sign (meaning)	Value	Unit
i (current)	7	$A = C\ s^{-1}$
N (coil turns)	300	
a (side of a square coil/2)	0.18	m
d (distance between coils/2)	1.089	m
θ (angle)	0–90	Deg.
μ_0 (permeability in vacuum)		$T\ Am^{-1}$
M (magnetization)	95 500	$A\ m^{-1}$
r (radius of magnet)	0.0005	m
h (length of magnet)	0.002	m

2.2. The structure of the jellyfish-like mini-robot

The structure of the jellyfish-like mini-robot is shown in figure 3. The robot consists of a main body with four fins, four neodymium permanent magnets, and a buoyant head in the center of the body. The robot body is 17 mm long and 0.5 mm thick. The cylindrical magnets with 1 mm diameter and 2 mm length are attached to the ends of the fins. In order to reduce the robot size to a microscale, the PDMS molding technique could be used. However, it would be difficult to attach the permanent magnets and the buoyant parts to the microscale robot body. In addition, the hydrodynamics could provide a dominant effect in the motion of the microscale robot. The main goal of this paper is not the miniaturization of the robot size but the demonstration of the jellyfish-like swimming mini-robot. Therefore, the size of the robot body was restricted to 17 mm, and other parameters (magnitude, frequency and waveform of the coil input current) were optimized.

Generally, jellyfish move by squeezing their bodies so that jets of water from the bottom of their bodies are pushed out; this causes the jellyfish to be propelled forward

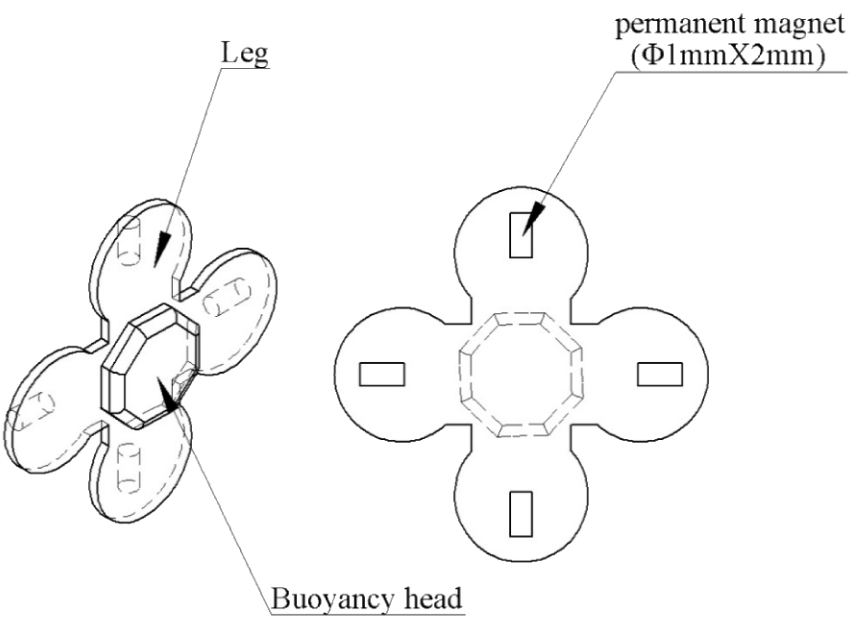

Figure 3. Structure of the jellyfish-like robot.

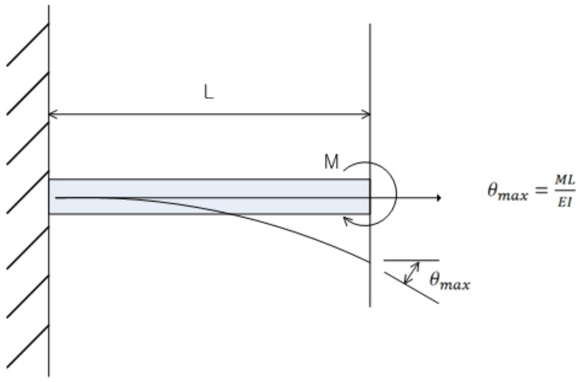

Figure 4. Deflection of the cantilever.

[1, 13–15]. The uniform magnetic field of the EMA coil system in the desired direction generates a moment on the magnets at the ends of the fins, and the moment torque causes a synchronous deflection of the fins. In addition, when the uniform magnetic field disappears, the fins will be restored to their original positions by the fins' elasticity. These bending and recovering motions propel the jellyfish-like robot.

As shown in figure 4, if we assume that the fins of the jellyfish robot are cantilevers, the relationship between the applied torque and the deflection angle is given as

$$M = \frac{EI}{L}\theta_{\max} \tag{5}$$

where M denotes the applied torque, E is Young's modulus, I is the moment of inertia, L the length of the cantilever, and $\theta_{\max}$ the maximum deflection angle of the cantilever. Therefore, when the deflection angle of the cantilever is given, the applied torque can be calculated.

2.3. Fabrication of the jellyfish-like mini-robot

The jellyfish-like mini-robot body was made from polydimethylsiloxane (PDMS), which has an elastic modulus varying according the ratio of the curing agents. It is a suitable material for the fabrication of a robot body requiring appropriate elasticity [16]. The ratio of the PDMS base polymer and the curing agent is approximately 15:1, and the elastic modulus of the fabricated robot body was measured as 12.23×10^6 N m^{-2} in a tensile test.

Figure 6. Fabricated jellyfish-like robot.

A molding technique was used to shape the robot body. As shown in figure 5, the mold consists of two smooth Teflon surfaces and a SUS plate with holes shaped like the robot's body. The Teflon surfaces were used for the separation of the robot body from the mold. Firstly, SUS plate was placed on the bottom Teflon surface. Secondly, PDMS solution (Sylgard 184 Silicone Elastomer Kit, Dow Corning), a mixture of PDMS prepolymer (Sylgard 184 A) and curing agent (Sylgard 184 B) with a 15:1 volume ratio, was slowly poured onto the SUS plate. Thirdly, the top Teflon surface was assembled on the SUS plate covered with the PDMS mixture. Fourthly, the molding assembly was placed in a heating chamber at 80 °C, for 3 h, and the PDMS structures in the assembly were cured. Finally, when the molding assembly was disassembled, the flexible PDMS robot body could be obtained. After the molding of the robot body, four magnets were attached to the

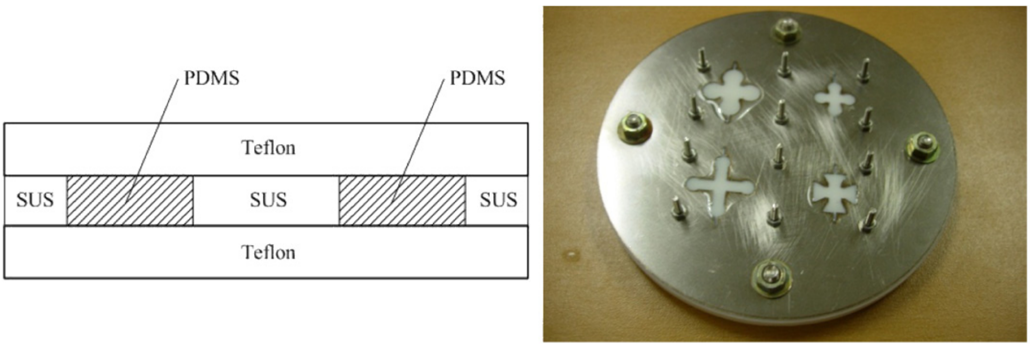

Figure 5. PDMS mold.

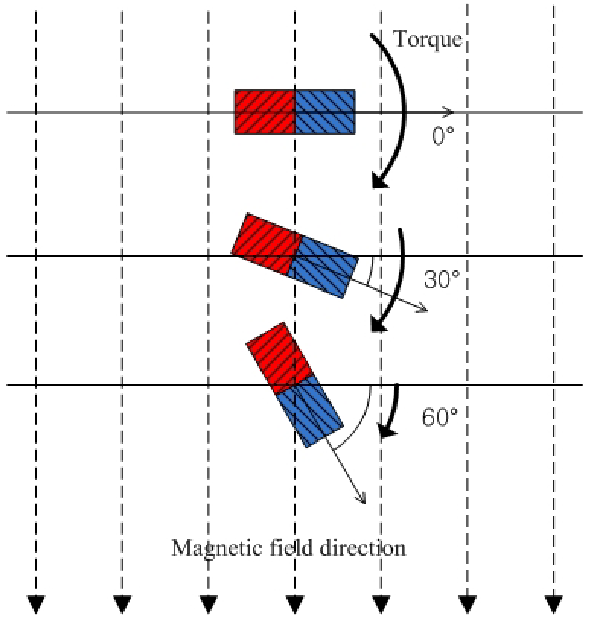

Figure 7. Torque differences according to the incident angles.

ends of the fins, and the buoyancy head, with disk-shaped Styrofoam, was assembled. The final jellyfish-like robot is shown in figure 6 and has a weight of 0.14 g.

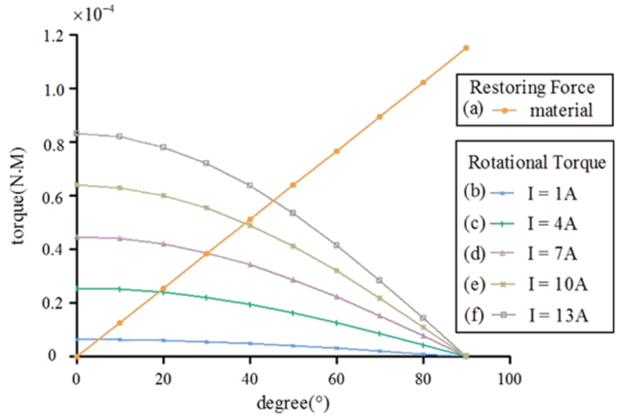

Figure 8. Torque of the material restoring force and rotational torques.

2.4. Deflection analysis of the jellyfish-like mini-robot

The deflection of the fins of the jellyfish-like mini-robot was estimated using equations (1) and (5). Firstly, assuming the fins of the jellyfish-like mini-robot as cantilevers, the relation of the applied torque and the deflection angle from equation (5) and figure 4, respectively, was calculated and this

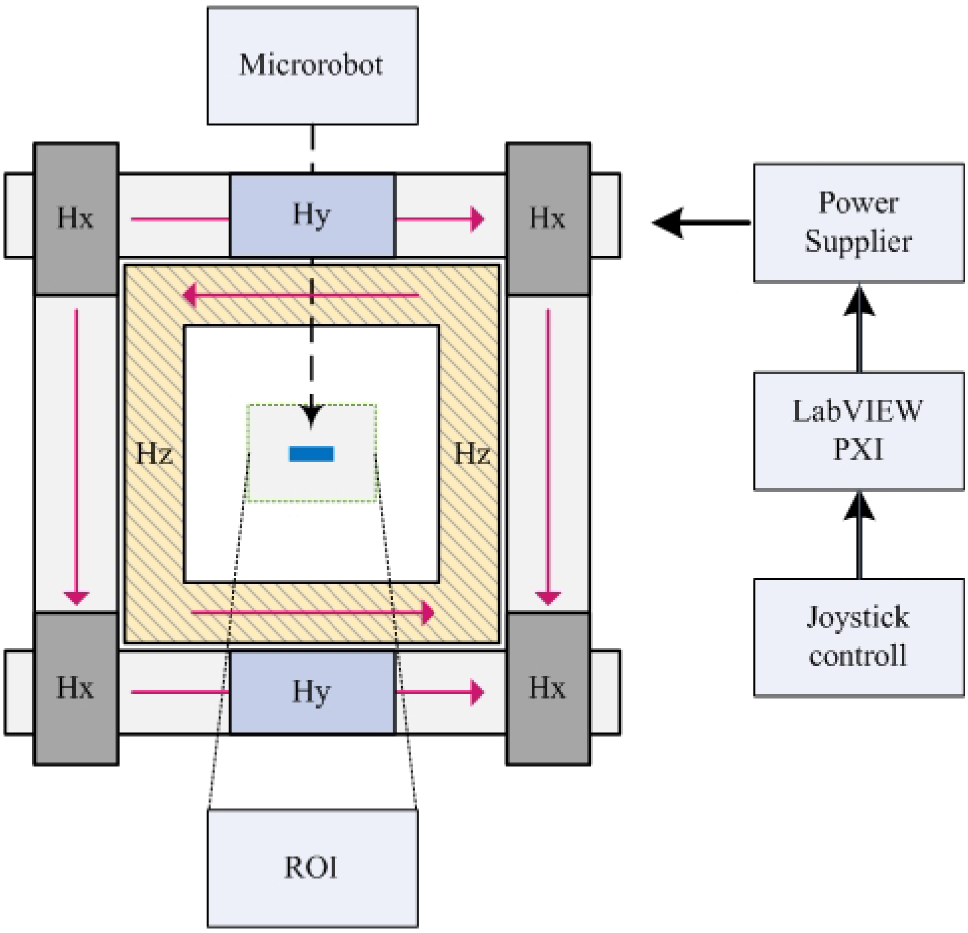

Figure 9. Schematic diagram of the experimental setup.

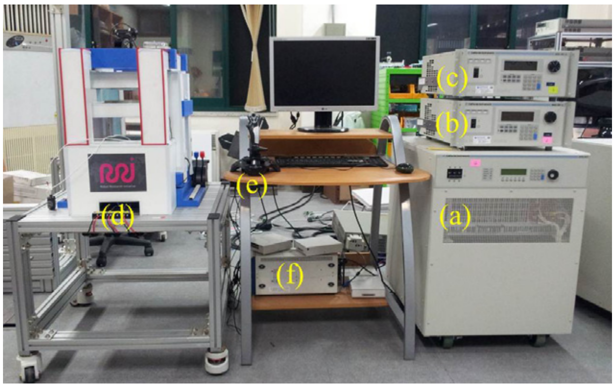

Figure 10. Experimental setup.

is plotted in figure 8(a). Secondly, the uniform magnetic field generated by the applied current in the Helmholtz coils was calculated. The uniform magnetic field induced the rotational torques of the magnets in the mini-robot fins, which are calculated using equation (1). As shown figure 7, a rotational torque could be changed according to the angle between the uniform magnetic field and the magnetization direction of the magnet. On the basis of the parameters of the EMA system in table 2, the rotational torque according to the change of included angles was calculated by using equation (1) and is plotted in figures 8(b)–(f) [17].

Force equilibria occurred at the crossing points between the relation of the applied torque and the deflection angle (figure 8(a)) and the rotational torques generated by the EMA system (figures 8(b)–(f)). Therefore, the deflection angles of the robot fins due to input currents could be estimated. For example, when the applied input current is 13 A, the deflection angle is about 47°, and the generated torque is about 0.6×10^{-4} N m.

3. Experiments

3.1. The experimental setup

The schematic diagram of the experimental setup is shown in figure 9. It consists of three pairs of Helmholtz coils, power suppliers, LabVIEW, the PXI controller, and a conventional joystick. The waveform and the frequency of the applied input current could be changed by using LabVIEW and the PXI controller, and the moving direction of the robot could be controlled by using a conventional joystick. For a test bed for the jellyfish-like robot, a cube-type bath cube of one-sided length of 8 mm was prepared, and the bath was filled with salt water in order to increase the buoyancy.

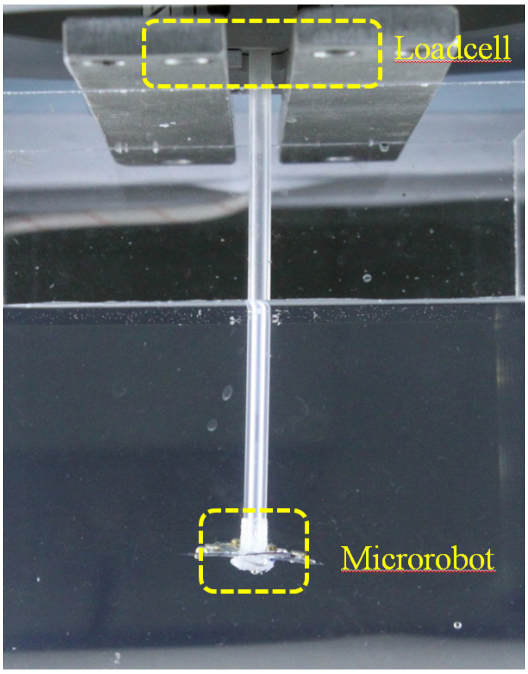

Figure 12. Measurement of the propulsion force.

Figure 10 shows the overall experimental setup, where (a)–(c) are the power suppliers (California Instruments MX15 and 300IXs), (d) is the three-axis Helmholtz coil system, (e) is the conventional joystick, and (f) is the PXI controller.

3.2. Basic actuation experiments with the jellyfish-like robot

We executed the bending test on the fins of the robot using the EMA system. As the input current of the EMA system was increased, the bending deformations of the fins were also increased. The currents were increased as 0, 1, 4, 7, 10, 13 A and the bending angles were increased as shown in figure 11. The initial bending angle, at 0 A input current, was believed

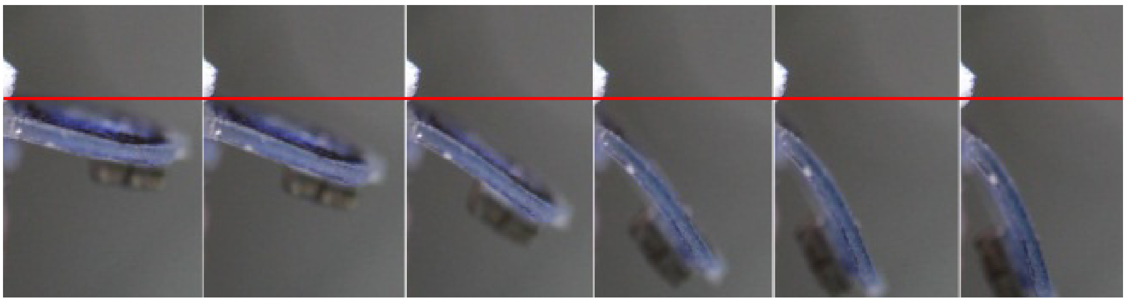

Figure 11. Deflection of the robot's fin (0, 1, 4, 7, 10, 13 A).

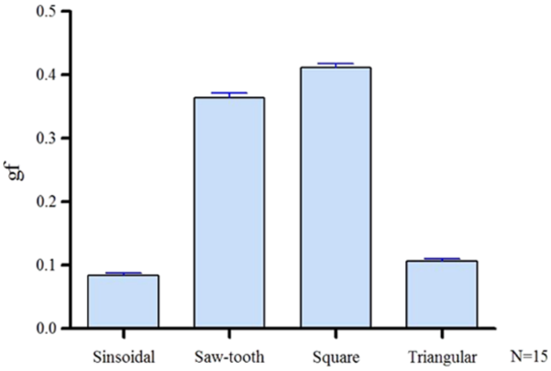

Figure 13. Comparison of effects of the waveform.

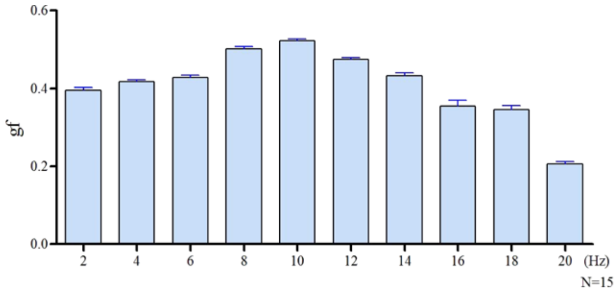

Figure 14. Comparison of the effects of frequency.

to be caused by the weight of the magnet. When the initial bending was considered, the maximum bending angle at 13 A was approximately 50°–60°. This experimental result was similar to the result of the deflection analysis in section 2.4. On the basis of the deflection of the fins of the robot in figure 11, it is expected that the propulsion motion of jellyfish can be mimicked by the jellyfish-like robot.

Secondly, the propulsion force of the jellyfish-like mini-robot could be measured. As shown in figure 12, the robot was connected to a load cell, and the null adjustment of the load cell was executed before the measurement of the propulsion force. Therefore, when the robot was actuated by the EMA system, the propulsion force of the robot could be measured. The effect of the waveform of the input current on the propulsion force was tested. We used four kinds of waveforms: sinusoidal, sawtooth, square, and triangular waves. These waveforms are closely related to the motions of the robot fins. Figure 13 shows the propulsion force of the robot according to the different waveforms. The input current of the square waveform generated the maximal propulsion force for the robot. Our proposed jellyfish-like swimming mini-robot could acquire propulsion force from the squeezing motion of the fins, such as in the downstroke of the flapping of birds. Like in the upstroke in the flapping, the fins of the robot returned to their initial posture. For the large propulsion force of the robot, a fast squeeze motion is necessary. Compared with other waveforms, the square wave has rapid fluctuations and regular durations at maximum and minimum values. These characteristics of the square wave resulted in large and rapid deflections of the fins and maximal propulsion force in the robot was generated.

The influence of the actuating frequency of the fins was tested. For the input current of the EMA system, the square waveform was utilized, and the frequency of the square wave was changed from 2 to 20 Hz. The propulsion force of the robot according to the actuating frequency was measured; see figure 14. When the frequency of the input current is about 10 Hz, the robot displays maximum propulsion force.

3.3. 3D locomotion of the jellyfish-like mini-robot

Through the bending and the propulsion force tests of the jellyfish-like robot, the appropriate waveform (square wave) and frequency (10 Hz) of the input current to the EMA system were found. However, for realistic motion of the jellyfish-like robot, we used a 3 Hz square wave as the actuating current

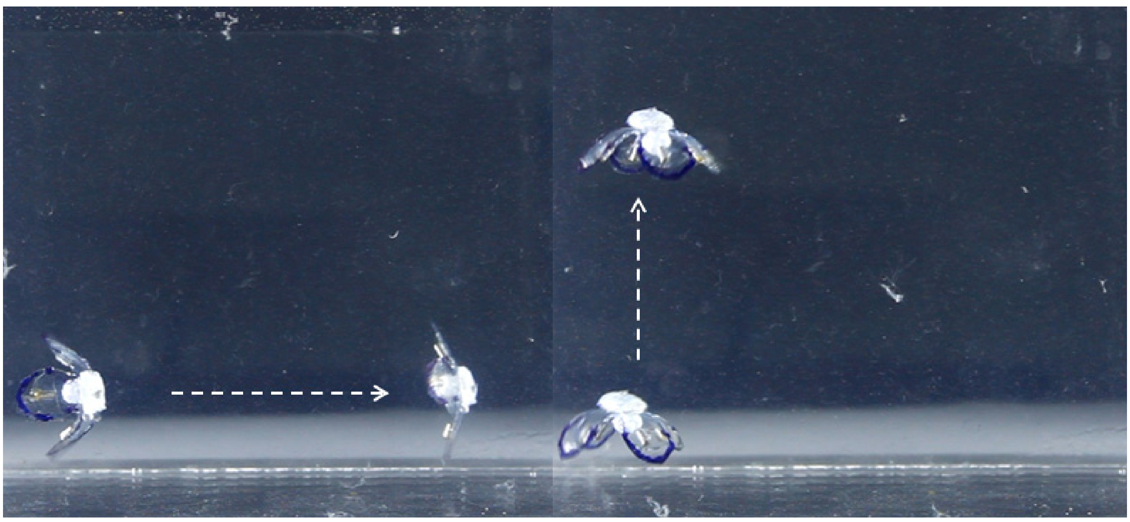

Figure 15. Horizontal (left) and vertical (right) locomotion of the jellyfish-like robot.

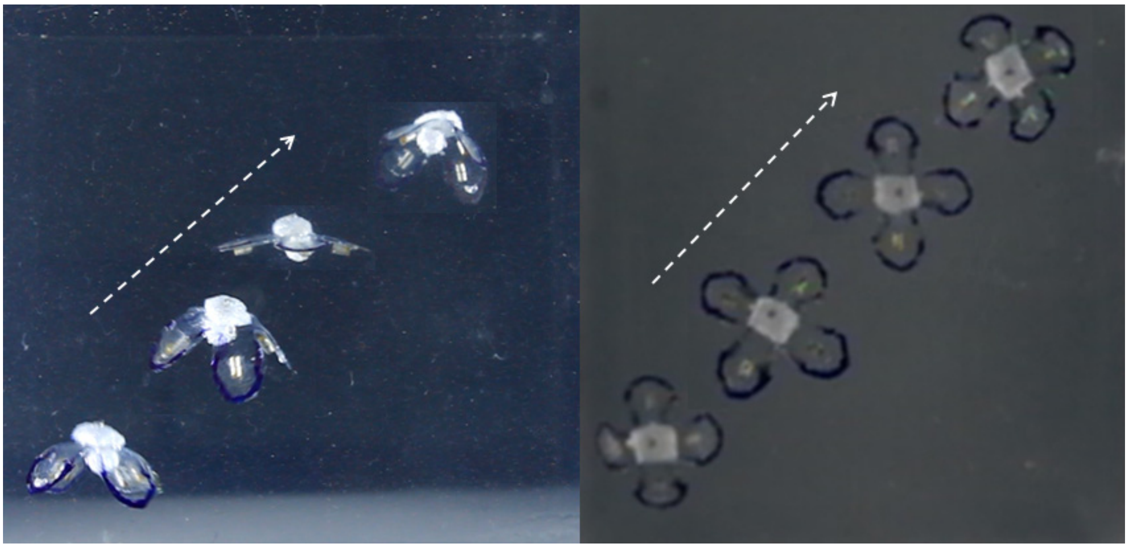

Figure 16. Side view (left) and top view (right) of the 3D locomotion of the jellyfish-like robot.

input. On the basis of these basic tests, 3D locomotion of the jellyfish-like mini-robot was realized.

To demonstrate the 3D locomotion of the robot, two kinds of basic locomotion tests were executed. Figure 15 shows horizontal and vertical locomotion results for the jellyfish-like robot. These locomotion results showed the basic locomotion of the robot in 3D space.

Finally, the free swimming motion of the jellyfish-like mini-robot was tested, and figure 16 shows a side and a top view of the robot. These results demonstrated the free swimming locomotion of the jellyfish-like mini-robot in 3D space. The swimming motion of the robot was found to appropriately imitate the motion of a real jellyfish.

4. Conclusion

This paper proposed a jellyfish-like mini-robot for a 3D space controlled by an external magnetic field, generated by three pairs of Helmholtz coils. The robot was designed and fabricated to mimic the motion of a real jellyfish. Through various basic tests of the robot, the 10 Hz square-type waveform was found to be appropriate for the actuating input current of the EMA system. Finally, 3D locomotion of the jellyfish-like mini-robot, using a 3 Hz square input current, was demonstrated. The swimming motion of the robot was similar to the motion of a real jellyfish. The proposed jellyfish-like mini-robot could be regarded as a swimming robot prototype for fluidic environments, such as the cerebral ventricle of the brain. Therefore, we expect that the proposed robot could be applied in medical applications, e.g. as a capsule endoscope, a clot-collecting device in a blood vessel, or a swimming robot for drug delivery.

Acknowledgments

This work was supported by the National Research Foundation of Korea (NRF) and a grant funded by the Korea government (MEST; No. 2011-0009975).

References

[1] Kim B K, Kim D H, Jung J H and Park J O 2005 A biomimetic undulatory tadpole robot using ionic polymer–metal composite actuators *Smart Mater. Struct.* **14** 1579–85

[2] McGovern S T, Spinks G M, Xii B, Alicil G, Truong V and Wallace G G 2008 Fast bender actuators for fish-like aquatic robots *Proc. SPIE* **6927** 6927IL

[3] Shi L, Asaka K and Guo S 2010 A novel of jellyfish-like biomimetic microrobot *The 2010 IEEE/ICME Int. Conf. Complex Medical Engineering* pp 277–81

[4] Yeom S W and Oh I K 2009 A biomimetic jellyfish robot based on ionic polymer metal composite actuators *Smart Mater. Struct.* **18** 085002

[5] Guo S, Sawamoto J and Pan Q 2005 A novel type of microbot for biomedical application *2005 IEEE/RSJ Int. Conf. Intelligent Robots and System* pp 1047–52

[6] Zhang L, Abbott J J, Dong L, Kratochvil B E, Bell D and Nelson B J 2009 Artificial bacterial flagella : fabrication and magnetic control *Appl. Phys. Lett.* **94** 94–6

[7] Kósa G, Jakab P, Jólesz F and Hata N 2008 Swimming capsule endoscope using static and RF magnetic field of MRI for propulsion *2008 IEEE Int. Conf. on Robotics and Automation* pp 2922–7

[8] Byun D H, Choi J H, Cha K R, Park J O and Park S H 2011 Swimming microrobot actuated by two pairs of Helmholtz coils system *Mechatronics* **21** 357–64

[9] Yu C S, Choi H C, Park J O and Park S H 2009 Three dimensional locomotive microrobot with electromagnetic actuation system *2009 IEEE/RSJ Int. Conf. on Intelligent Robots and Systems* pp 540–5

[10] Choi J H, Choi H C, Cha K G, Park J O and Park S H 2009 Two-dimensional locomotive permanent magnet using electromagnetic actuation system with two pairs stationary coils *2009 IEEE Int. Conf. on Robotics and Biomimetics (ROBIO)* pp 1166–71

[11] Li T T 2004 *Tri-axial Square Helmholtz Coil for Neutron EDM Experiment* (Hong Kong: Chinese University of Hong Kong)

[12] Alamgir A K M, Fang J, Gu C and Han Z 2005 Square Helmholtz coil with homogeneous field for magnetic measurement of longer HTS Tapes *Physica* C **424** 17–24

[13] McHenry M J and Jed J 2003 The ontogenetic scaling of hydrodynamics and swimming performance in jellyfish (Aurelia aurita) *J. Exp. Biol.* **206** 4125–37

[14] Hsieh W H and Chen T I 2010 On the resonance analysis for compliant bionic jellyfishes *Sci. China Technol. Sci.* **53** 2976–82

[15] Tortora G, Caccavaro S, Valdastri P, Menciassi A and Dario P 2010 Design of an autonomous swimming miniature robot based on a novel concept of magnetic actuation *2010 IEEE Int. Conf. on Robotics and Automation* pp 1592–7

[16] Armani D, Liu C and Aluru N 1999 Re-configurable fluid circuits PDMS by elastomer micromachining *IEEE Int. Conf. on Micro Electro Mechanical Systems* pp 222–7

[17] Jeong S M, Choi H C, Choi J H, Yu C S, Park J O and Park S H 2010 Novel electromagnetic actuation (EMA) method for 3-dimensional locomotion of intravascular microrobot *Sensors Actuators* A **161** 118–25